

Eduardo L. V. Costa
João Batista Borges
Alexandre Melo
Fernando Suarez-Sipmann
Carlos Toufen Jr
Stephan H. Bohm
Marcelo B. P. Amato

Bedside estimation of recruitable alveolar collapse and hyperdistension by electrical impedance tomography

Received: 26 November 2007
Accepted: 4 February 2009
Published online: 3 March 2009
© Springer-Verlag 2009

E. L. V. Costa · J. B. Borges ·
A. Melo · C. Toufen Jr · S. H. Bohm ·
M. B. P. Amato
Respiratory Intensive Care Unit,
University of São Paulo School
of Medicine, São Paulo, Brazil

F. Suarez-Sipmann
Intensive Care Unit, Fundación Jiménez
Días-Capio, Madrid, Spain

M. B. P. Amato (✉)
Laboratório de Pneumologia LIM09,
Faculdade de Medicina da USP,
Av. Dr Arnaldo 455 (Sala 2206, 2nd floor),
São Paulo 01246-903, Brazil
e-mail: amato@unisys.com.br
Tel.: +55-11-30617361

Abstract Objective: To present a novel algorithm for estimating recruitable alveolar collapse and hyperdistension based on electrical impedance tomography (EIT) during a decremental positive end-expiratory pressure (PEEP) titration.

Design: Technical note with illustrative case reports.

Setting: Respiratory intensive care unit. **Patient:** Patients with acute respiratory distress syndrome. **Interventions:** Lung recruitment and PEEP titration maneuver. **Measurements and results:** Simultaneous acquisition of EIT and X-ray computerized tomography (CT) data. We found good agreement (in terms of amount and spatial location) between the collapse estimated by EIT and CT for all levels of PEEP. The optimal PEEP values detected by EIT for patients 1 and 2 (keeping lung collapse <10%) were 19 and 17 cmH₂O,

respectively. Although pointing to the same non-dependent lung regions, EIT estimates of hyperdistension represent the functional deterioration of lung units, instead of their anatomical changes, and could not be compared directly with static CT estimates for hyperinflation. **Conclusions:** We described an EIT-based method for estimating recruitable alveolar collapse at the bedside, pointing out its regional distribution. Additionally, we proposed a measure of lung hyperdistension based on regional lung mechanics.

Keywords Electrical impedance tomography · Computed tomography · Acute lung injury · Acute respiratory distress syndrome · Lung recruitment · Positive end-expiratory pressure · Mechanical ventilation

Introduction

Compelling evidence about the deleterious effects of mechanical ventilation has accumulated, suggesting that both lung collapse and alveolar hyperdistension can cause or perpetuate lung injury [1–4]. Protective ventilatory strategies have been proposed to minimize this injury [3–6].

Careful titration of positive end-expiratory pressure (PEEP) following maximal lung recruitment [7–9] effectively reverses existing collapse and prevents further alveolar closure. Due to disease heterogeneity, however, the airway pressure required to maintain some regions of

the lung fully open frequently leads to significant alveolar hyperdistension in others, even with low tidal volumes [10, 11]. Thus, a monitoring tool capable of estimating the location and amount of alveolar collapse and hyperdistension during PEEP titration would be invaluable at the bedside.

Electrical impedance tomography (EIT) is a noninvasive, radiation-free real-time imaging method that measures global and regional changes in lung volumes [12–15]. In this article, we introduce a novel EIT-based algorithm that estimates recruitable alveolar collapse and hyperdistension during a decremental PEEP titration.

Methods

Electrical impedance tomography

EIT data were acquired using the impedance tomograph Enlight[®] (Dixtal, São Paulo, Brazil), which produces 50 images/s using 32 electrodes. Images based on a 3D finite element model were reconstructed, assuming a 6-cm-wide cross-section of the thorax, and plotted in a matrix containing 860 valid pixels from a total of 1,024 (32 × 32). Output pixel values represent percent changes in local impedance as compared to a reference taken at the beginning of the acquisition.

Concept of estimating recruitable alveolar collapse

Calculating pixel compliance

To calculate the compliance of a compartment inside the respiratory system, it is necessary to know the incoming amount of air (*local tidal volume*) and its corresponding *driving pressure* (inspiratory minus expiratory pressure). Driving pressure can easily be obtained in a pressure-controlled mode if both end-inspiratory and end-expiratory flows reach zero. At zero flow, alveolar and proximal airway pressures attain equilibrium so that plateau pressure (P_{plateau}) and PEEP can be substituted for inspiratory and expiratory alveolar pressures, respectively. Local tidal volume, on the other hand, can be estimated by EIT

on a pixel by pixel basis, considering that it correlates very well with local impedance variations (ΔZ) [12–15]. We, therefore, calculate pixel compliance as

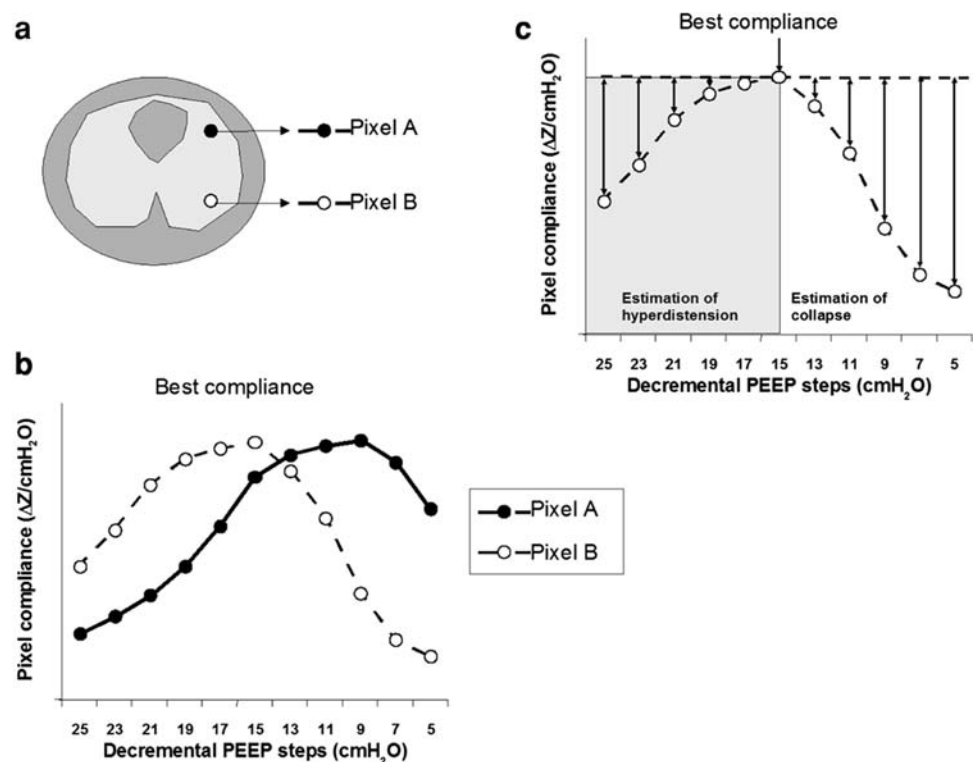
$$\text{Compliance}_{\text{pixel}} = \frac{\Delta Z}{P_{\text{plateau}} - \text{PEEP}} \quad (1)$$

Estimating recruitable alveolar collapse

During PEEP titration [7–9], there might be relief of hyperdistension in some regions of the lung while others collapse progressively, the former leading to increased, the latter to decreased lung compliance. When monitoring the overall lung compliance across PEEP steps, we measure the net result of these two antagonistic phenomena, usually producing a dampened, non-informative curve. As opposed to global parameters, EIT tracks changes in ventilation in smaller lung regions, thus making it possible to assess the spatial distribution of these concurrent and opposing phenomena. Also, within each pixel, opposite behaviors can be observed according to the range of PEEP studied (Fig. 1).

In the concept to be proposed here we assume, as in previous investigations [16, 17], that the best compliance of a lung compartment reflects the number of functional lung units in that region, which, once open, have equivalent compliances. Thus, from the decrease in pixel compliance, inferences can be made as to the relative

Fig. 1 **a** Sketch of two pixels in different locations with respect to the gravitational vector (*closed circles* non-dependent, *open circles* dependent pixel) and **b** their respective pixel compliances during a decremental PEEP titration. **c** General concept behind the estimation of hyperdistension and collapse; the *arrows* represent the loss of compliance (relative to maximum pixel compliance) at each PEEP level, which was used to calculate both the parameters



amount of alveolar collapse (amount of units lost) within that pixel [16, 17]. We devised an EIT-based algorithm that estimates cumulated alveolar collapse during a decremental PEEP titration, after maximally recruiting the lung by

1. calculating pixel compliance at every PEEP step according to Eq. 1;
2. determining at a certain PEEP step the percent change in compliance for each pixel in relation to its “best compliance” (Fig. 1c), according to the formula:

$$\begin{aligned} \text{Collapse}_{\text{pixel}} (\%) \\ = \frac{(\text{Best compliance}_{\text{pixel}} - \text{Current compliance}_{\text{pixel}}) \times 100}{\text{Best compliance}_{\text{pixel}}} \end{aligned} \quad (2)$$

where $\text{Best compliance}_{\text{pixel}}$ is the highest compliance value for each pixel across all PEEP steps, and $\text{Collapse}_{\text{pixel}} (\%)$ is set to 0 if the $\text{Best compliance}_{\text{pixel}}$ has not yet been achieved for that pixel.

3. finally estimating the cumulated collapse for the entire lung at each PEEP step as the weighted average of $\text{Collapse}_{\text{pixel}}$, where the weighting factor is the best pixel compliance, which is assumed to indicate the functional size of the lung compartment represented by a certain EIT pixel:

$$\begin{aligned} \text{Cumulated collapse} (\%) \\ = \frac{\sum_{\text{Pixel}=1}^{860} (\text{Collapse}_{\text{pixel}} (\%) \times \text{Best compliance}_{\text{pixel}})}{\sum_{\text{Pixel}=1}^{860} (\text{Best compliance}_{\text{pixel}})} \end{aligned} \quad (3)$$

Concept of estimating alveolar hyperdistension

During a decremental PEEP trial, the high initial PEEP levels lead to lung hyperdistension, which can be assessed as a percent decrease in pixel compliance in relation to its peak value ($\text{Best compliance}_{\text{pixel}}$) measured at lower PEEPs. Although original in terms of its regional characterization, this concept bears similarities with Bersten’s attempts to measure overdistension [18] by quantifying deviations from the most linear portion of the pressure–volume curve, where compliance is maximal. Similarly to the estimation of recruitable alveolar collapse, we estimated alveolar hyperdistension according to the formula:

$$\begin{aligned} \text{Hyperdistension}_{\text{pixel}} (\%) \\ = \frac{(\text{Best compliance}_{\text{pixel}} - \text{Current compliance}_{\text{pixel}}) \times 100}{\text{Best compliance}_{\text{pixel}}} \end{aligned} \quad (4)$$

where $\text{Hyperdistension}_{\text{pixel}} (\%)$ is set to 0 if the $\text{Best compliance}_{\text{pixel}}$ has already been achieved for that pixel (Fig. 1c):

Cumulated hyperdistension (%)

$$= \frac{\sum_{\text{Pixel}=1}^{860} (\text{Hyperdistension}_{\text{pixel}} \times \text{Best compliance}_{\text{pixel}})}{\sum_{\text{Pixel}=1}^{860} (\text{Best compliance}_{\text{pixel}})} \quad (5)$$

Case report

We report two cases of hypoxic respiratory failure due to severe pneumonia. The first patient was a 38-year-old man whose chest radiography showed diffuse opacities. During baseline ventilation with pure oxygen and PEEP of 10 cmH₂O, arterial oxygen tension (PaO₂) was 167 mmHg and reached a maximum of 476 mmHg after attaining maximal lung recruitment with PEEP level of 45 cmH₂O.

The second patient was a 47-year-old man with right inferior lobe pneumonia. His PaO₂ was 204 mmHg at PEEP of 10 cmH₂O with 100% oxygen, and reached a maximum of 237 mmHg after unsuccessful lung recruitment. Both patients were submitted to a decremental PEEP titration in 5-min steps of 2 cmH₂O, starting at a PEEP of 25 cmH₂O. During the procedure, we kept the driving pressure constant at 8 cmH₂O. Multislice computed tomography (CT) scanning (LightSpeed, GE Healthcare, Milwaukee, WI, USA) during an expiratory pause was performed at minute 4 of each step, whereas EIT data and global mechanics were acquired continuously. PEEP values of 19 and 17 cmH₂O were the lowest pressures capable of limiting EIT-based recruitable collapse to 10% or less for patients 1 and 2, respectively. At those PEEP levels, PaO₂ was 556 and 216 mmHg, respectively. Figure 2 shows the comparison of percent mass of collapsed lung tissue and hyperinflation estimated by CT versus collapse and hyperdistension estimated by EIT [9, 19].

Discussion

In the present study, we described a novel EIT-based method for estimating recruitable alveolar collapse and hyperdistension. In two patients in whom we titrated PEEP while simultaneously acquiring EIT and CT data, we showed good agreement between the recruitable collapse estimated by EIT and increase in collapse in relation to minimum CT collapse for all levels of PEEP. The comparison between CT and EIT estimations of recruitable lung collapse was straightforward because both CT and EIT methods of estimating lung collapse assumed that alveolar collapse was an ON/OFF phenomenon (anatomically and functionally). We also showed that hyperdistension was identified by EIT in the same

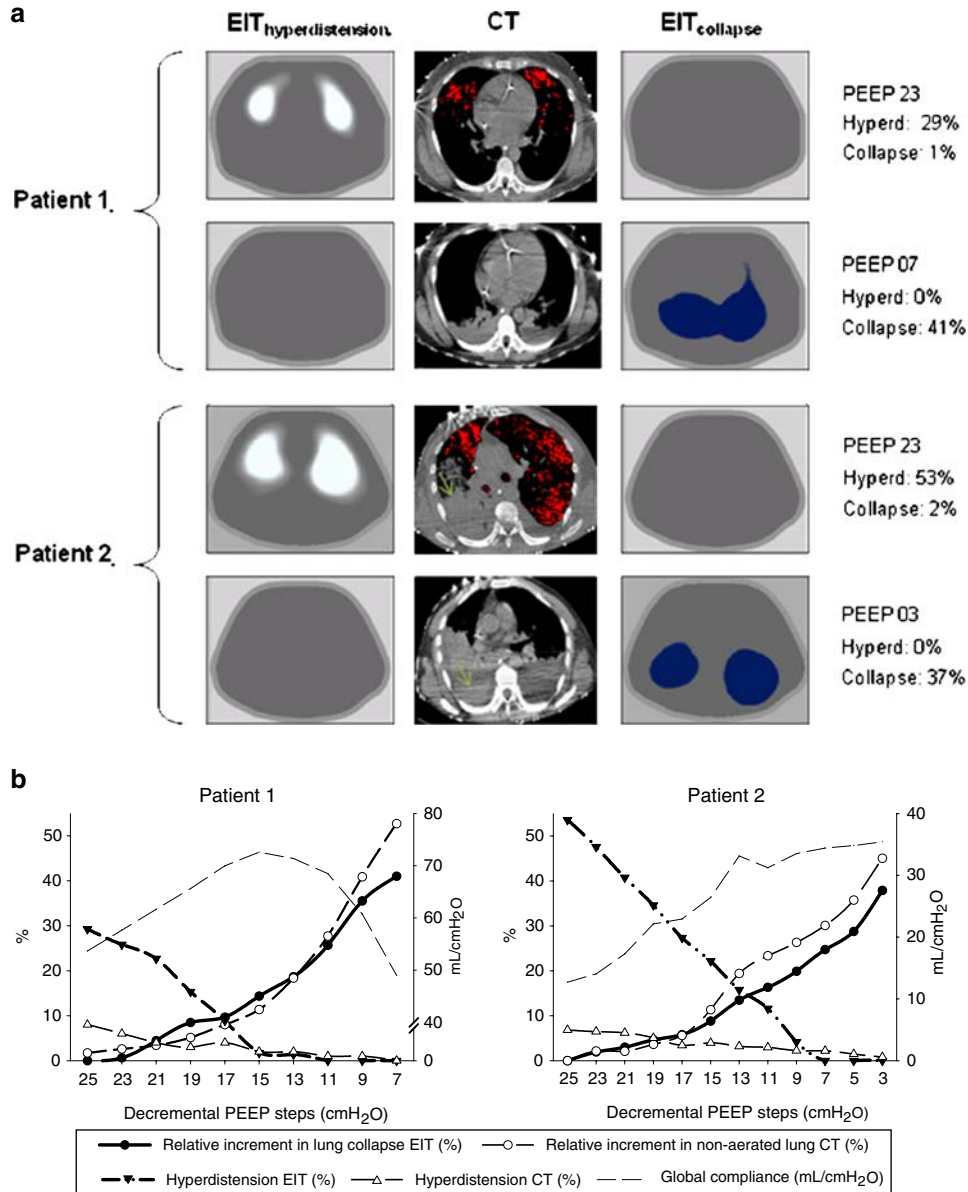


Fig. 2 a Summary of the PEEP titration process for patients 1 and 2 with EIT images showing hyperdistension on the *left* and cumulative collapse on the *right column*, for two representative PEEP levels. Note the decrease in hyperdistension and increase in collapse as PEEP is reduced. For comparison, we show CT images taken at the respective PEEP levels. All CT pixels presenting densities <-850 HU were marked in *red*. Note that EIT images of collapse just represent zones of re-collapse during the titration process, not including the non-recruitable zones (*arrows*). Slice thickness is 1 cm on CT images and approximately 7 cm on EIT images. **b** Line graphs showing the increments (%) of collapsed tissue from the post-recruitment condition till the lowest possible

PEEP. The collapse in CT was calculated as percent increment of lung mass showing densities >-100 HU, and represented as *open circles*; EIT is represented by *closed circles*. Patient 2 had a high initial amount of collapse as measured by CT (58%) even at the highest PEEP level (first decremental PEEP step), consistent with the unsuccessful recruitment. The *open circles* with the fine *dotted line* represent the CT estimation of collapse excluding the non-recruitable pneumonia. EIT-based estimates of hyperdistension (*closed triangles*) are also shown, in contrast with hyperinflation (*open triangles*) measured by CT (defined as the percent lung mass showing densities <-850HU). The behavior of global compliance is presented as a *dotted line* only

non-dependent regions marked as hyperinflated by CT. Nevertheless, EIT hyperdistension was systematically higher than CT hyperinflation, despite a reasonable

correlation between both quantities ($R^2 = 0.85$ and 0.95 , for patients 1 and 2). This discrepancy existed because hyperdistension was a functional measure of alveolar

distension based on the departure from the linear elasticity of the lung parenchyma, while CT-derived hyperinflation was an ON/OFF phenomenon based on anatomical, static densities. Thus, a high parenchymal density at baseline could have rendered CT analysis insensitive (the hyperinflation threshold would hardly be exceeded), whereas the EIT estimation could still reveal excessive tissue stretch. Alternatively, distension of already hyperinflated pixels might have been missed by CT (once the density threshold was already exceeded), whereas the EIT could still reveal further deterioration of pixel compliance.

Using the concept of functional imaging described by Frerichs [14, 20], and combining this information with airway pressures, we were able to estimate regional compliances. The changes in pixel compliance during a decremental PEEP trial were used to estimate collapse and hyperdistension. These changes were weight-averaged according to each pixel's maximal compliance to compensate for different amounts of alveolar units contained within each voxel.

Our method has some limitations: first, all calculations assume that the driving pressure at the airway opening is a good surrogate for the local transpulmonary driving pressure. This assumption has been discussed extensively in CT studies assessing local lung mechanics [21]. It is based on the premise that the lung is a freely deformable body within the chest wall and thus, chest wall compliance affects the lung as a whole. In our particular case, this assumption also requires that the chest wall compliance is constant across the titration process. Therefore, changes in pixel compliance reflect changes in lung behavior only. By these reasonable assumptions, heterogeneities caused by gravity are expected to create a gradient of pleural pressures and alveolar size in proportion to lung weight, but not a gradient of driving pressures. Therefore, our algorithm considers driving pressure to be constant for all voxels, irrespective of their location along the gravitational vector.

As we follow the gravity vector inside the lung, the increasing offsets in expiratory transpulmonary pressures cause a “right shift” in the local pressure–volume curves, with little effect on its overall shape. Consequently, maximal compliance values are not affected by the anterior–posterior position, although the PEEP at which it occurs displays large variations (Fig. 1b). Thus, by taking the maximal compliance of the entire PEEP range as the reference *best compliance* for each pixel (Fig. 1c), we can adequately compensate for such offsets in transpulmonary pressures.

Second, beside these possible inter-voxel heterogeneities, we have to consider intra-voxel heterogeneities, i.e., voxels containing both open and closed alveoli at a given alveolar pressure. With the early loss of some alveolar

units, the theoretically possible absolute maximum of voxel compliance might not be reached during the titration process, leading to underestimation of both Best compliance_{pixel} and alveolar collapse. Nevertheless, we believe that by subdividing the chest anterior-posteriorly into 32 regions we were able to minimize gravitational influences—the main source of lung heterogeneity in ARDS patients [22].

Additionally, EIT measurements are influenced not only by the amount of air but also by the fluid content of the thorax. The changes in intrathoracic blood that occur during a PEEP titration maneuver might produce significant offsets in impedance levels. However, our calculations of pixel compliance only take into account the tidal variation in impedance within each PEEP step. Consequently, the influence of fluid shifts should be minimal, considering that tidal variations in pleural pressure are low.

Finally, as exemplified in case report 2 (Fig. 2), maximal recruitment leading to an “open lung condition” is necessary to provide precise collapse estimation. This requirement exists because EIT is not capable of measuring absolute amounts of alveolar collapse and our estimation method assumes aeration to be 100% after a maximal recruitment maneuver. Even though incomplete lung recruitment interferes with the estimation of the absolute amount of collapse, we believe that this is of lesser importance. For the care of an individual patient, EIT will still provide the amount of collapse in relation to the minimum possible collapse after lung recruitment and physicians will be able to titrate PEEP within alveolar pressure limits considered clinically acceptable.

Other investigators have shown that EIT can be used to follow changes in lung volume during PEEP titration maneuvers [23–26] and assess local mechanics in acute lung injury [27]. We, however, propose a novel method that uses regional volume allied with the driving pressure to estimate lung collapse and hyperdistension.

In conclusion, we described a bedside method based on EIT for estimating recruitable alveolar collapse and its regional distribution. During a decremental PEEP trial, the location and quantification of collapse detected by EIT agreed well with that calculated from CT data. Additionally, we proposed a measure of lung hyperdistension based on regional lung mechanics. Although this measure may disclose focal hyperdistension, spatially coinciding with hyperinflated areas on CT, it should not be compared directly to CT-hyperinflation because they have different meanings.

Acknowledgments Financial support by grants from “Fundação de Amparo à Pesquisa do Estado de São Paulo (FAPESP)”, São Paulo State Research Support Foundation and “Financiadora de Estudos e Projetos (FINEP)”, Studies and Projects Financial Support Provider and to Dixtal Biomédica, Ltda.

References

1. Tremblay LN, Slutsky AS (1998) Ventilator-induced injury: from barotrauma to biotrauma. *Proc Assoc Am Physicians* 110:482–488
2. Plötz FB, Slutsky AS, van Vught AJ, Heijnen CJ (2004) Ventilator-induced lung injury and multiple system organ failure: a critical review of facts and hypotheses. *Intensive Care Med* 30:1865–1872
3. ARDSNet (2000) Ventilation with lower tidal volumes as compared with traditional tidal volumes for acute lung injury and the acute respiratory distress syndrome. The acute respiratory distress syndrome network. *N Engl J Med* 342:1301–1308
4. Amato MBP, Barbas CS, Medeiros DM, Magaldi RB, Schettino GP, Lorenzi-Filho G, Kairalla RA, Deheinzelin D, Munoz C, Oliveira R, Takagaki TY, Carvalho CR (1998) Effect of a protective-ventilation strategy on mortality in the acute respiratory distress syndrome. *N Engl J Med* 338:347–354
5. Villar J, Kacmarek RM, Pérez-Méndez L, Aguirre-Jaime A (2006) A high positive end-expiratory pressure, low tidal volume ventilatory strategy improves outcome in persistent acute respiratory distress syndrome: a randomized, controlled trial. *Crit Care Med* 34:1311–1318
6. Ranieri VM, Suter PM, Tortorella C, De Tullio R, Dayer JM, Brienza A, Bruno F, Slutsky AS (1999) Effect of mechanical ventilation on inflammatory mediators in patients with acute respiratory distress syndrome: a randomized controlled trial. *JAMA* 282:54–61
7. Suarez-Sipmann F, Böhm SH, Tusman G, Pesch T, Thamm O, Reissmann H, Reske A, Magnusson A, Hedenstierna G (2007) Use of dynamic compliance for open lung positive end-expiratory pressure titration in an experimental study. *Crit Care Med* 35:214–221
8. Borges JB, Carvalho CRR, Amato MBP (2006) Lung recruitment in patients with ards. *N Engl J Med* 355:319–320 (author reply 321–322)
9. Borges JB, Okamoto VN, Matos GFJ, Caraméz MPR, Arantes PR, Barros F, Souza CE, Victorino JA, Kacmarek RM, Barbas CSV, Carvalho CRR, Amato MBP (2006) Reversibility of lung collapse and hypoxemia in early acute respiratory distress syndrome. *Am J Respir Crit Care Med* 174:268–278
10. Terragni PP, Rosboch G, Tealdi A, Corno E, Menaldo E, Davini O, Gandini G, Herrmann P, Mascia L, Quintel M, Slutsky AS, Gattinoni L, Ranieri VM (2007) Tidal hyperinflation during low tidal volume ventilation in acute respiratory distress syndrome. *Am J Respir Crit Care Med* 175:160–166
11. Grasso S, Stripoli T, De Michele M, Bruno F, Moschetta M, Angelelli G, Munno I, Ruggiero V, Anaclerio R, Cafarelli A, Driessen B, Fiore T (2007) Ardsnet ventilatory protocol and alveolar hyperinflation: role of positive end-expiratory pressure. *Am J Respir Crit Care Med* 176:761–767
12. Victorino JA, Borges JB, Okamoto VN, Matos GFJ, Tucci MR, Caraméz MPR, Tanaka H, Sipmann FS, Santos DCB, Barbas CSV, Carvalho CRR, Amato MBP (2004) Imbalances in regional lung ventilation: a validation study on electrical impedance tomography. *Am J Respir Crit Care Med* 169:791–800
13. Frerichs I, Hinz J, Herrmann P, Weisser G, Hahn G, Dudykevych T, Quintel M, Hellige G (2002) Detection of local lung air content by electrical impedance tomography compared with electron beam ct. *J Appl Physiol* 93:660–666
14. Frerichs I, Hahn G, Schiffmann H, Berger C, Hellige G (1999) Monitoring regional lung ventilation by functional electrical impedance tomography during assisted ventilation. *Ann NY Acad Sci* 873:493–505
15. Adler A, Amyot R, Guardo R, Bates JH, Berthiaume Y (1997) Monitoring changes in lung air and liquid volumes with electrical impedance tomography. *J Appl Physiol* 83:1762–1767
16. Hickling KG (2001) Best compliance during a decremental, but not incremental, positive end-expiratory pressure trial is related to open-lung positive end-expiratory pressure: a mathematical model of acute respiratory distress syndrome lungs. *Am J Respir Crit Care Med* 163:69–78
17. Frazer DG, Weber KC, Franz GN (1985) Evidence of sequential opening and closing of lung units during inflation-deflation of excised rat lungs. *Respir Physiol* 61:277–288
18. Bersten AD (1998) Measurement of overinflation by multiple linear regression analysis in patients with acute lung injury. *Eur Respir J* 12:526–532
19. Hedenstierna G, Tokics L, Strandberg A, Lundquist H, Brismar B (1986) Correlation of gas exchange impairment to development of atelectasis during anaesthesia and muscle paralysis. *Acta Anaesthesiol Scand* 30:183–191
20. Frerichs I, Hahn G, Hellige G (1996) Gravity-dependent phenomena in lung ventilation determined by functional EIT. *Physiol Meas* 17(Suppl 4A):A149–A157
21. Simon BA, Christensen GE, Low DA, Reinhardt JM (2005) Computed tomography studies of lung mechanics. *Proc Am Thorac Soc* 2(517–521):506–507
22. Gattinoni L, Pelosi P, Vitale G, Pesenti A, D'Andrea L, Mascheroni D (1991) Body position changes redistribute lung computed-tomographic density in patients with acute respiratory failure. *Anesthesiology* 74:15–23
23. Frerichs I, Dargaville PA, Dudykevych T, Rimensberger PC (2003) Electrical impedance tomography: a method for monitoring regional lung aeration and tidal volume distribution? *Intensive Care Med* 29:2312–2316
24. Meier T, Luepschen H, Karsten J, Leibecke T, Großherr M, Gehring H, Leonhardt S (2008) Assessment of regional lung recruitment and derecruitment during a peep trial based on electrical impedance tomography. *Intensive Care Med* 34:543–550
25. Lindgren S, Odenstedt H, Olegård C, Söndergaard S, Lundin S, Stenqvist O (2007) Regional lung derecruitment after endotracheal suction during volume- or pressure-controlled ventilation: a study using electric impedance tomography. *Intensive Care Med* 33:172–180
26. Erlandsson K, Odenstedt H, Lundin S, Stenqvist O (2006) Positive end-expiratory pressure optimization using electric impedance tomography in morbidly obese patients during laparoscopic gastric bypass surgery. *Acta Anaesthesiol Scand* 50:833–839
27. Hinz J, Gehoff A, Moerer O, Frerichs I, Hahn G, Hellige G, Quintel M (2007) Regional filling characteristics of the lungs in mechanically ventilated patients with acute lung injury. *Eur J Anaesthesiol* 24:414–424